Article

SOURCE
DATA

TRANSPARENT
PROCESS

THE
EMBO
JOURNAL

Contact-dependent growth inhibition induces high levels of antibiotic-tolerant persister cells in clonal bacterial populations

Anirban Ghosh[†], Özden Baltekin[†], Marcus Wäneskog, Dina Elkhalifa, Disa L Hammarlöf, Johan Elf (iD) & Sanna Koskiniemi[*] (iD)

Abstract

Bacterial populations can use bet-hedging strategies to cope with rapidly changing environments. One example is non-growing cells in clonal bacterial populations that are able to persist antibiotic treatment. Previous studies suggest that persisters arise in bacterial populations either stochastically through variation in levels of global signalling molecules between individual cells, or in response to various stresses. Here, we show that toxins used in contact-dependent growth inhibition (CDI) create persisters upon direct contact with cells lacking sufficient levels of CdiI immunity protein, which would otherwise bind to and neutralize toxin activity. CDI-mediated persisters form through a feedforward cycle where the toxic activity of the CdiA toxin increases cellular (p)ppGpp levels, which results in Lon-mediated degradation of the immunity protein and more free toxin. Thus, CDI systems mediate a population density-dependent bet-hedging strategy, where the fraction of non-growing cells is increased only when there are many cells of the same genotype. This may be one of the mechanisms of how CDI systems increase the fitness of their hosts.

Introduction

Clonal populations of bacteria often show remarkable phenotypic variability in gene expression (Elowitz *et al*, 2002; Ozbudak *et al*, 2002) and growth rate (Balaban *et al*, 2004). Such population heterogeneity can be useful for division of labour between cells (Ackermann, 2015) or as a bet-hedging strategy where short time

fitness is sacrificed in a fraction of the cells to ensure survival of the population upon rapid changes to harsh conditions (Veening *et al*, 2008). For example, non-growing cells in a heterogeneous bacterial population are able to tolerate antibiotic treatment, a phenomenon referred to as persistence (Balaban *et al*, 2004; Keren *et al*, 2004a). Persisters consist of heterogeneous populations of cells with transient phenotypes that allow them to survive antibiotic exposure through different mechanisms (Amato *et al*, 2013; Amato & Brynildsen, 2015; Pu *et al*, 2016). When the concentration of antibiotics in the host subside, for example at the end of therapy, the non-growing persisters can cause a relapse of the infection (Butler, 2011).

Even though the persistence phenomenon has been known for decades (Bigger, 1944), the mechanisms of persister formation have only recently been investigated. Isolation of high persistence (*hip*) mutants indicated that persisters constitute a pre-existing subpopulation of cells that form stochastically in bacterial populations (Moyed & Bertrand, 1983). The first identified and most excessively studied *hip* alleles were identified in the *hipBA* locus, which encodes a toxin–antitoxin (TA) system (Moyed & Bertrand, 1983; Korch *et al*, 2003). When the levels of the HipA toxin exceed a threshold in single cells, growth is arrested (Balaban *et al*, 2004). HipA phosphorylates an amino acid close to the active site of the glutamyl-tRNA synthetase enzyme (GltX), which in turn inhibits aminoacylation, inducing a conserved bacterial response to nutrient starvation known as the stringent response (Germain *et al*, 2013). During the stringent response in *Escherichia coli*, RelA and SpoT synthesize (p)ppGpp, an alarmone that directly interacts with RNA polymerase and thereby changes the expression of more than 500 genes, decelerating growth (Durfee *et al*, 2008; Traxler *et al*, 2008). One widely accepted model suggests that persister subpopulations arise from what appears to be stochastic cell-to-cell variation in the level of the signalling molecule (p)ppGpp. Cells with sufficiently high (p)ppGpp concentrations activate the Lon protease (Kuroda *et al*, 2001; Maisonneuve *et al*, 2013), which can degrade antitoxins and other unfolded proteins. Degradation of antitoxins results in unneutralized toxins that become free to corrupt essential processes in the cell, ultimately entailing growth arrest and entry into a

---

Department of Cell and Molecular Biology, Uppsala University, Uppsala, Sweden
*Corresponding author. Tel: +46 18 4716683; E-mail: sanna.koskiniemi@icm.uu.se
[†]These authors contributed equally to this work

persister state (Appendix Fig S1A; Keren *et al*, 2004b; Maisonneuve *et al*, 2011, 2013; Vazquez-Laslop *et al*, 2006). A recent study suggested an addition to this model where increased ATP levels in some cells, rather than low (p)ppGpp levels, result in a subpopulation of cells tolerant to antibiotics (Conlon *et al*, 2016; Shan *et al*, 2017). Interestingly, increased (p)ppGpp levels also result in expression of the type I HokB toxin, mediated by the GPTase Obg. HokB dissipates the proton motive force and depletes cellular ATP levels (Verstraeten *et al*, 2015; Appendix Fig S1A), suggesting that stochastic variation in (p)ppGpp could influence the ATP levels in cells and that the two models are not necessarily exclusive of one another.

Like intracellular TA systems, contact-dependent growth inhibition (CDI) systems also inhibit cell growth through toxin-dependent mechanisms (Aoki *et al*, 2005, 2010). During CDI, cells encoding CDI systems express a two-component system, where the β-barrel transporter CdiB exports and displays the CdiA protein on the cell surface (Ruhe *et al*, 2013a). CdiA proteins are modular, comprising of an N-terminal domain of triple stranded beta helix structure, a receptor binding domain and a C-terminal toxin domain (CdiA-CT) (Ruhe *et al*, 2013a, 2017). Upon contact with cells carrying the correct species-specific receptor [β-barrel assembly machine protein A, BamA (Ruhe *et al*, 2013b), outer membrane protein OmpC (Beck *et al*, 2016) or small-molecule transporter Tsx, respectively, for different CdiA binding domains (Ruhe *et al*, 2017)], the CdiA protein binds to its cognate receptor, undergoes a proteolytic cleavage event and delivers its toxic CT into target cells (Webb *et al*, 2013; Fig EV1A). To avoid auto-inhibition, cells with CDI systems express an immunity protein, CdiI, that prevents toxicity by forming a tight complex with the CdiA-CT (Fig EV1A and B; Aoki *et al*, 2010, 2005). Different toxins have distinct toxic activities. For example, the CdiA-CT from EC93 (CdiA-CT^{EC93}) acts as an ionophore toxin dissipating the proton motive force (Fig EV1A, lower left panel; Aoki *et al*, 2009), whereas the CdiA-CT from uropathogenic *E. coli* 536 (CdiA-CT^{UPEC536}) and enterohemorrhagic *E. coli* 869 (CdiA-CT^{EC869}) are nucleases that cleave tRNAs (Fig EV1A, upper and lower right panels; Aoki *et al*, 2010; Diner *et al*, 2012; Jones *et al*, 2017). A peculiar attribute suggested for CDI is that toxin delivery is limited to its own species, which allows CDI-positive cells to deliver toxins between one another, but limits competitiveness in populations with mixed bacterial species (Ruhe *et al*, 2013b). Thus, the evolutionary benefit of inhibiting the growth specifically of the same species is unclear.

Cells undergoing CDI mediated by CdiA-CT^{EC93} show a reversible downregulation of steady-state ATP levels. Inhibited cells can restart growth up to 6 h into growth arrest, upon induced expression of the immunity protein (Aoki *et al*, 2009). This shows that CDI can be reversible and results in inhibition of growth rather than cell death. However, whether CDI contributes to population heterogeneity in terms of growth has not yet been investigated. Here, we show that CDI increases the fraction of persisters in bacterial populations. These persisters are formed in the presence of CdiI through a feedforward cycle in which the toxins induce the stringent response, resulting in Lon-mediated degradation of the CDI immunity proteins and growth arrest (Fig EV1B). In contrast to previously identified toxins that contribute to persister formation, CDI only creates non-growing cells upon cell-to-cell contact. Cell-to-cell contacts are more common at high cell densities; for example, both stationary phase and in biofilms are conditions where persisters are

found frequently (Spoering & Lewis, 2001; Keren *et al*, 2004a; Maisonneuve *et al*, 2013; Gutierrez *et al*, 2017). But in contrast to previously identified systems involved in generation of persisters, CDI functions as a quorum sensing system where an increased fraction of persisters is generated only when there are many cells of the same genotype. Thus, this suggests that it is cell number and not nutrient availability that determines when more persisters are formed through CDI. As the contact-dependent mechanism facilitates persister formation only when there are many cells of the same genotype, increasing the fraction of non-growing cells will have little effect on the growth of the entire population. This makes density-dependent regulation of persister formation through CDI a highly rational bet-hedging strategy that does not limit population expansion.

Results

CDI toxins increase bacterial survival to antibiotics

Cells inhibited by the CdiA-CT^{EC93} toxin show characteristics typical of persister cells (Aoki *et al*, 2009), yet whether CDI systems contribute to antibiotic tolerance has not been tested. To examine a possible role of CDI in generation of persisters, we removed the *cdiBAI* loci in the *E. coli* strain EC93 where CDI was first discovered (Aoki *et al*, 2005). EC93 cells deleted for the CDI loci had 5–10 times fewer survivors than wild-type EC93 cells after 3 h of treatment with bactericidal antibiotics [ciprofloxacin, CIP (Fig 1A and Appendix Fig S2A) or cefotaxime, CEF (Fig EV2A and Appendix Fig S3A)], suggesting that CDI systems could be involved in the generation of persisters. For clarity, we use the term survival instead of persister frequency when referring to figures throughout the paper. Similarly, although to lesser extent, uropathogenic *E. coli* UPEC 536 cells lacking the toxic C-terminal domain and cognate *cdiI* gene (*cdiA*$^{ΔCT–I}$) had ~50% fewer survivors after CIP (Fig 1B and Appendix Fig S2B) and CEF (Fig EV2B and Appendix Fig S3B) treatment. This strain has previously been shown to express very little *cdiBAI* during laboratory conditions (Aoki *et al*, 2010), which could explain why only a small difference could be observed between cells with and without CDI toxin. The C-terminal domains of CdiA proteins from various *E. coli* strains encode toxins with different activity and we therefore wanted to investigate if the ability to increase the fraction of non-growing cells in a population was limited to the CdiA toxin from EC93, or if other CdiA toxins also contribute to persister formation when expressed. We chose two additional CdiA toxins from other *E. coli* strains and used a previously described simplified system to test this. In these constructs, the entire CDI locus from *E. coli* strain EC93, expressing *cdiBAI* with either the native EC93 toxin (CdiA-CT-I^{EC93}), the UPEC536 toxin (CdiA-CT-I^{UPEC536}), or the EC869 main toxin (CdiA-CT-I^{EC869}), and their respective cognate immunity protein were cloned into a medium-copy vector downstream of the native EC93 promoter (Fig EV1A; Aoki *et al*, 2010, 2005). These plasmids as well as an empty vector control were transferred to *E. coli* MG1655 cells. For all experiments, the empty vector control was used to determine how the presence of the plasmid in the absence of CDI affected persister formation. Inhibitor strains carrying the entire *cdiBAI* locus on a medium-copy number plasmid were exposed to CIP or CEF,
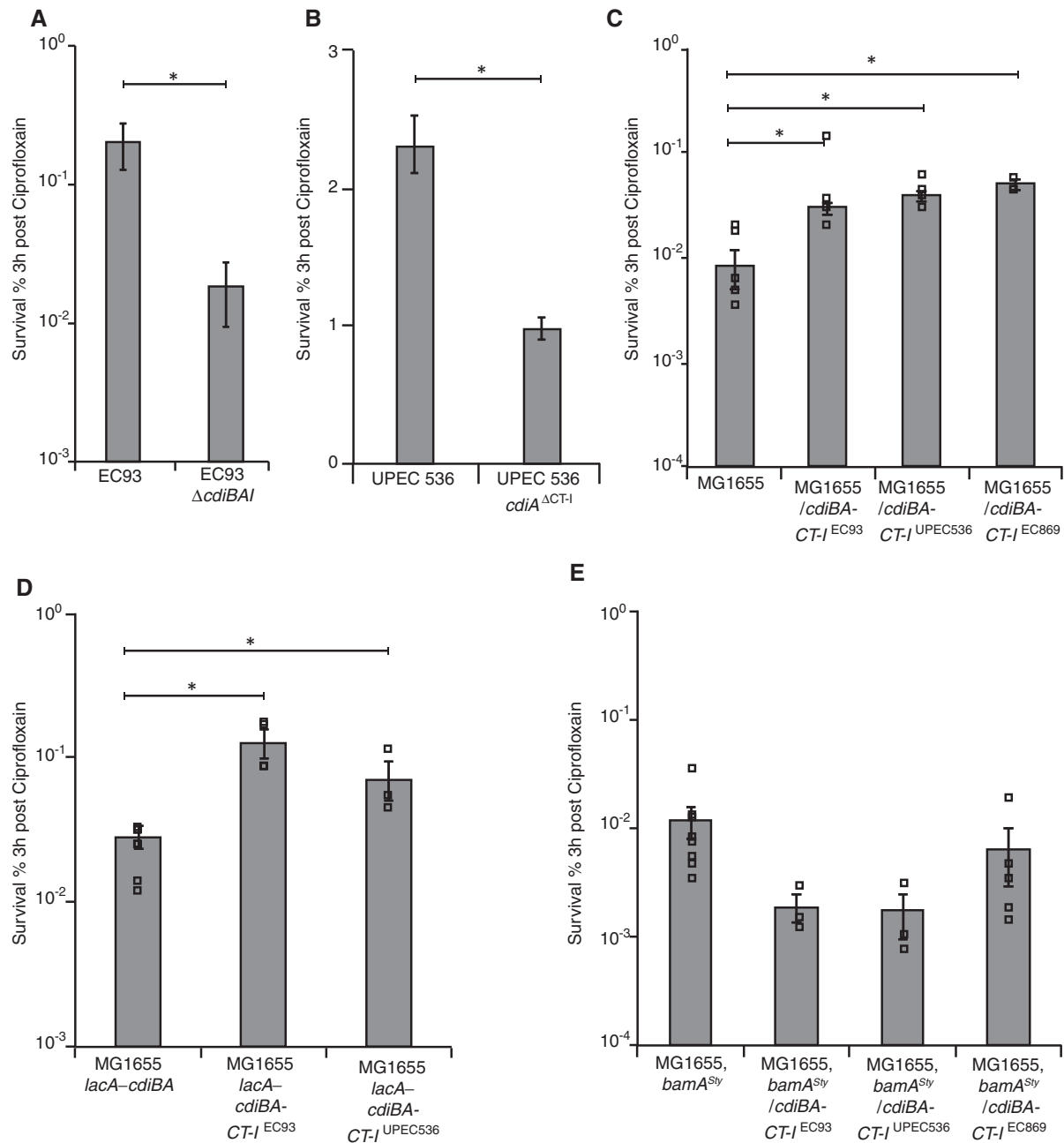
Figure 1. Contact-dependent growth inhibition systems increase antibiotic tolerance.

Average survival of exponentially growing *Escherichia coli* cells after 3 h of ciprofloxacin (CIP) treatment.

A   EC93 cells with or without *cdiBAI* loci (*n* = 5).
B   Uropathogenic *E. coli* 536 (UPEC 536) cells with or without CdiA C-terminal toxin and immunity (*cdiA*$^{\Delta CT-I}$) (*n* = 7).
C   MG1655 cells with empty, *cdiBA-CT-I*^{EC93}, *cdiBA-CT-I*^{UPEC536} or *cdiBA-CT-I*^{EC869} plasmids (*n* = 5, 4, 4, 3).
D   MG1655 cells with chromosomally encoded *cdiBA*, *cdiBA-CT-I*^{EC93} or *cdiBA-CT-I*^{UPEC536} (*n* = 7, 4, 3).
E   MG1655 *bamA*^{Sty} cells with empty, *cdiBA-CT-I*^{EC93}, *cdiBA-CT-I*^{UPEC536} or *cdiBA-CT-I*^{EC869} plasmids (*n* = 8, 3, 3, 5).

Data information: Scales are logarithmic for (A, C–E) and linear for (B). Error bars represent s.e.m., and *n*-values indicate biological replicates. Statistical significance was determined using Mann–Whitney *U*-test. *$P < 0.05$.
Source data are available online for this figure.

and survivors were counted. MG1655 cells with *cdi*-loci (either CdiA-CT-I^{EC93}, CdiA-CT-I^{UPEC536}, or CdiA-CT-I^{EC869} toxins) displayed 6–10 (CIP) (Fig 1C and Appendix Fig S2C) and 10–100 times (CEF)

(Fig EV2C and Appendix Fig S3C) more survivors than the empty vector control strain after 3 h of antibiotic treatment. As CDI toxins are delivered from one cell to another upon cell-to-cell contacts, the

number of molecules delivered is expected to be low also when the delivering cell has multiple copies of the CDI loci. However, most CDI loci are found on the bacterial chromosome, that is, in one copy per cell. To test if the presence of CDI loci on the chromosome increased persister formation in MG1655 [as was observed in EC93 (Fig 1A)], we inserted the entire *cdiBAI* loci from the CdiA-CT-I^{EC93} and CdiA-CT-I^{UPEC536} vectors downstream of the *lacA* gene on the MG1655 chromosome. To verify that these chromosomal copies of the *cdiBAI* genes were able to mediate CDI, we mixed these strains with MG1655 cells marked with a chromosomal chloramphenicol (*cat*) resistance marker (*lacA-cat*) and observed viability over time. MG1655 cells with chromosomally encoded *cdiBA-CT-I*^{EC93} or *cdiBA-CT-I*^{UPEC536} loci inhibited the growth of MG1655 cells similarly as observed with the plasmid based constructs described previously (Appendix Fig S4A and B), suggesting that these new constructs were active in CDI. Interestingly, MG1655 cells with chromosomally encoded *cdiBA-CT-I*^{EC93} or *cdiBA-CT-I*^{UPEC536} loci showed 10-fold increase in persisters to CIP (Fig 1D and Appendix Fig S2D), compared to control cells encoding *cdiB* and the N-terminal part of *cdiA* (no toxin and immunity). This suggests that the copy number of the genes does not affect the frequency of persisters in the population. Thus, our data show that CDI toxins with different activity confer significantly increased frequencies of persisters. To further confirm that the observed increase in persisters was due to delivery of toxins between cells and not simply due to expression of the *cdiBAI* genes, the plasmid-encoded *cdiBAI genes with CT-I* from EC93, UPEC 536 or EC869 were transformed into cells expressing a non-cognate BamA receptor protein from *Salmonella typhimurium* LT2 (*bamA*^{Sty}). Previous studies have shown that delivery of CdiA toxins does not occur to cells expressing this non-cognate BamA^{Sty} receptor (Ruhe *et al*, 2013b, 2015, 2016), but to confirm that this strain truly was resistant to CdiA toxin delivery, we competed the MG1655 strain with *bamA*^{Sty} against MG1655 expressing *cdiBA-CT-I*^{EC93} or *cdiBA-CT-I*^{UPEC536}. The growth of MG1655 target cells with *bamA*^{Sty} was not affected by co-culturing with strains expressing CdiA toxins from EC93 or UPEC 536 (Appendix Fig S4C), to be compared to the 2-log inhibition observed in *bamA* wild-type MG1655 target cells (Appendix Fig S4B). Interestingly, cells with the non-cognate receptor BamA^{Sty} and the plasmid-encoded *cdiBAI* genes with toxin and immunity from EC93, UPEC 536 or EC869 did not survive antibiotic exposure better than cells with empty vector (Fig 1E and Appendix Fig S2E for CIP and Fig EV2D and Appendix Fig S3D for CEF), suggesting that the CDI-mediated increase in persisters depends on delivery of CdiA toxin and is not due to expression of the CdiBAI proteins *per se*.

Cells inhibited by CdiA toxins become persister cells

Cells with *cdiBAI* loci show increased fractions of persisters in the bacterial population, but whether it is CDI toxicity *per se* that entails antibiotic tolerance is not known. To test if cells inhibited by CDI toxins survive antibiotic exposure better than uninhibited cells, EC93 cells lacking CdiA-CT and CdiI (*cdiA*$^{\Delta CT-I}$, RIF^R) were challenged by wild-type EC93 cells [able to inhibit cells lacking CdiI (*cdiA*$^{\Delta CT-I}$)] or EC93 cells lacking the CdiA-CT toxin and immunity (*cdiA*$^{\Delta CT-I}$) [unable to inhibit cells lacking CdiI (*cdiA*$^{\Delta CT-I}$)]. After 15 min, the culture was treated with CIP, and

the number of surviving target cells was monitored by plating on LB plates supplemented with rifampicin (RIF) to select for target cells in the mixed population (Fig 2A). Inhibited EC93 cells survived antibiotic exposure (CIP) ~100 times better than the uninhibited control (Fig 2B and C). The EC93 toxin is an ionophore that dissipates the proton motive force (Aoki *et al*, 2009) and the only CDI toxin with this activity described so far, whereas most studied CDI toxins are nucleases. To test if also nuclease toxins increase survival to antibiotics in cells inhibited by the toxin, we used the vector-based systems described above (and shown in Fig EV1). *Escherichia coli* MG1655 cells expressing *cdiBAI* with CdiA-CT-I^{EC93} or CdiA-CT-I^{UPEC536} were added to otherwise isogenic *E. coli* MG1655 target cells without the *cdiBAI* locus, and thus *cdiI*. To differentiate the target cells from the inhibitors, the targets carry a chromosomal kanamycin resistance marker in *setB* that does not affect persister formation (Appendix Fig S5A and B). Target cells inhibited by either of the two CdiA toxins, CdiA-CT^{EC93} that dissipates the proton motive force or CdiA-CT^{UPEC536} that cleaves tRNA (Aoki *et al*, 2010), survived CIP and CEF exposure 1,000–10,000 times better than uninhibited target cells (Figs 2D, and EV3A and B). In contrast, target cells expressing the cognate immunity protein from a high-copy vector failed to form more survivors when challenged by cells expressing the toxin (Figs 2D, and EV3A and B). Thus, these data suggest that growth inhibition *per se*, rather than toxin delivery and other potential effects that the delivered toxin may have in the cell, increases antibiotic tolerance. To verify that the inhibited cells were indeed persisters, the cells from Fig 2D were regrown and treated with CIP when they reached exponential phase. Regrown survivors behaved like untreated cells, confirming that the survivors in our experiments were indeed persisters, and ruling out mutations resulting in antibiotic resistance (Appendix Fig S6). To test if the copy number and thus expression level of *cdiBAI* affected delivery-mediated persister formation in cells lacking *cdiI*, we used the strains where the entire CDI loci from the two vectors above was cloned in the MG1655 chromosome. Cells inhibited by chromosomally encoded CDI loci showed a 20- to 1,000-fold increase in survival to CIP (Fig 2E) similar, although to lesser extent, to what was observed for the multi-copy system. Thus, the copy number of CDI loci does seem to change CDI-induced persistence in cells with no *cdiI* immunity, in contrast to what was observed in the *cdiI*-positive populations (Fig 1C and D). An obvious difference between these two conditions is that in the *cdiI*-negative cells, every toxin delivered can arrest growth of the cell. In contrast, only cells where the CdiA toxin molecules outnumber the CdiI molecules will arrest growth of the *cdiI*-positive cells. As the fraction of persisters in *cdiI*-positive populations does not increase with increased production of CdiA molecules, it must be the CdiI levels that are different between individual cells. Thus, it is possible that some cells in the *cdiI*-positive populations are predisposed for persistence, with low CdiI levels, prior to CdiA toxin delivery, and that it is the number of such cells that limits the fraction of persisters that are formed by CDI under these conditions. The majority of previous studies on CDI have been performed with the vector-based systems described above (e.g. Aoki *et al*, 2005, 2008, 2009, 2010; Diner *et al*, 2012; Ruhe *et al*, 2013b, 2015; Beck *et al*, 2016), which is the reason we decided to use these constructs for the remainder of the study.
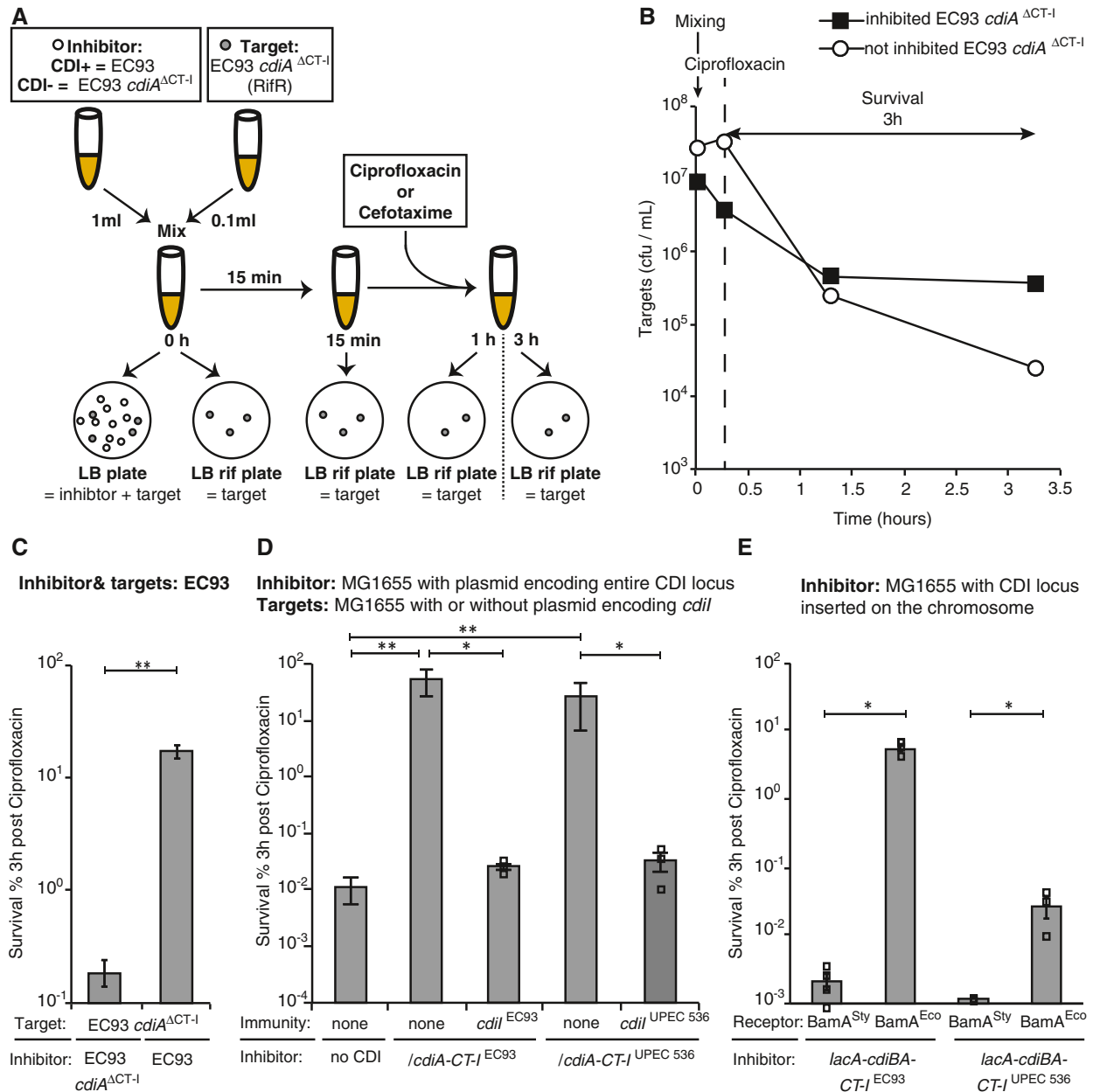
Figure 2. CdiA toxins induce antibiotic tolerance in growth-inhibited cells.

A Overview of experiment. EC93 inhibitor cells with or without CDI (EC93 $cdiA^{\Delta CT-I}$) were mixed with target cells lacking $cdiI$ (EC93 $cdiA^{\Delta CT-I}$) at a 10:1 ratio for 15 min prior to addition of antibiotics (CIP or CEF). The number of viable cells was monitored over time through plating on LB plates (measuring both inhibitor and target cells) and LB rifampicin plates (measuring target cells only). In the figure, only target plates are shown at later time points due to space restriction, but plating on both plates was done at all time points to control the presence of inhibitors in the mix.

B A representative experiment (included in C) where cells lacking CdiI (EC93 $cdiA^{\Delta CT-I}$) were co-cultured with wild-type EC93 cells (black squares) or with $cdiA^{\Delta CT-I}$ cells (white circles) cells for 15 min before treatment with CIP. Mixing is indicated by a vertical arrow and survival (plotted in C) by a horizontal arrow. Addition of CIP is indicated with a dashed line.

C Average survival of EC93 $cdiA^{\Delta CT-I}$ cells co-cultured with wild-type or $cdiA^{\Delta CT-I}$ EC93 cells, after 3 h of CIP treatment ($n = 6$).

D Average survival of MG1655 cells with or without immunity to the corresponding toxin ($cdiI^{EC93}$ or $cdiI^{UPEC536}$) co-cultured with empty vector, plasmid-encoded $cdiBA$-CT-I^{EC93}- or $cdiBA$-CT-$I^{UPEC536}$-positive inhibitor cells, after 3 h of CIP treatment. ($n = 10$ for empty vector and $cdiBA$-CT-I^{EC93}, $n = 8$ for $cdiBA$-CT-$I^{UPEC536}$ and $n = 3$ for immunity complemented targets).

E Average survival of wild-type or $bamA^{Sty}$ MG1655 cells co-cultured with chromosomally encoded $cdiBA$-CT-I^{EC93}- or $cdiBA$-CT-$I^{UPEC536}$-positive inhibitor cells, after 3 h of CIP treatment ($n = 4$ for $cdiBA$-CT-I^{EC93} and $n = 3$ for $cdiBA$-CT-$I^{UPEC536}$).

Data information: Error bars represent s.e.m. and n-values indicate biological replicates. Statistical significance was determined using Mann-Whitney U-test. Scales are logarithmic (C–E). *$P < 0.05$, **$P < 0.01$.
Source data are available online for this figure.

Growing and persister cells are targeted similarly by contact-dependent growth inhibition

A possible caveat in the experiments described above lies in the fact that CDI might target *either* only growing cells, or *both* growing and persister cells. This distinction is critical to correctly assess the survival of the inhibited population (Fig 2B), because exclusive targeting of growing cells would leave pre-existing persisters unaffected. To test if CDI targets growing and persister cells alike, cell growth was transiently arrested by treatment with serine hydroxamate (SHX, a serine analogue that inhibits serine-tRNA synthetase), thus mimicking amino acid starvation and inducing stringent response (Tosa & Pizer, 1971) before addition of inhibitor cells expressing CDI (for competitions), or only antibiotics (for persister assay) (Fig 3A). Clearly, CdiA-expressing cells inhibited SHX-treated and untreated target cells to the same extent (2 orders of magnitude within 3 h; Fig 3B, compare solid and striped bars). The SHX-treated cells displayed complete tolerance against CEF, showing that they represent bona fide persisters (Fig 3C). Taken together, these results suggest that CDI does not discriminate between growing and non-growing cells, confirming that the estimate of persisters in Fig 2 is correct.

CdiI immunity protein is degraded upon stringent response

In cells encoding a CDI system, the CdiI immunity protein binds tightly to its cognate toxin to protect from auto-inhibition (Aoki *et al*, 2010). So how could the presence of a CDI system infer toxicity to cells with immunity protein to increase persister frequencies? We hypothesized that the CdiA toxins increase the frequency of persisters in cells with CdiI because Lon degrades the immunity protein, as has been observed for antitoxins of several TA systems (Tsuchimoto *et al*, 1992; Van Melderen *et al*, 1994; Smith & Rawlings, 1998; Christensen *et al*, 2003, 2004), and asked if this in turn depends on (p)ppGpp production by RelA/SpoT and activation of the Lon protease via Ppk (Appendix Fig S1A and B; Maisonneuve *et al*, 2013). Plasmids with or without *cdi*-loci were transformed into strains lacking the two (p)ppGpp synthases, Δ*relA*, Δ*spoT*, or the protease Δ*lon*, and the resulting strains were tested for tolerance to antibiotics. Cells carrying plasmids with *cdi*-loci (*cdiBA-CT-I*[EC93] or *cdiBA-CT-I*[UPEC536]), but deleted for Δ*relA*, Δ*spoT*, or *lon*, did not survive CIP (Fig 4A and B, Appendix Fig S7A and B) treatment better than those carrying the empty vector. Lon protease also degrades the major cell-division inhibitor protein SulA, which is induced by antibiotics that target DNA (e.g. CIP). Thus, SulA accumulation in the absence of Lon could potentially affect the outcome of the experiment. However, cells carrying plasmids with *cdi*-loci (*cdiBA-CT-I*[EC93] or *cdiBA-CT-I*[UPEC536]), but deleted for *lon* did not survive exposure to antibiotics that target cell wall biosynthesis (CEF) better than those carrying the empty vector (Fig EV4A and Appendix Fig S8A). In addition, the assay was repeated in cells lacking *sulA* (Δ*lon*, Δ*sulA*). Similar to the *lon* mutants, double deletion cells with *cdi*-loci did not survive CIP (Fig 4C and Appendix Fig S7C) or CEF (Fig EV4B and Appendix Fig S8B) treatment better than the empty vector strain. To validate that Lon indeed was involved in the degradation of CdiI immunity proteins, the *in vivo* decay of a C-terminally HA-tagged CdiI immunity protein was monitored in exponentially
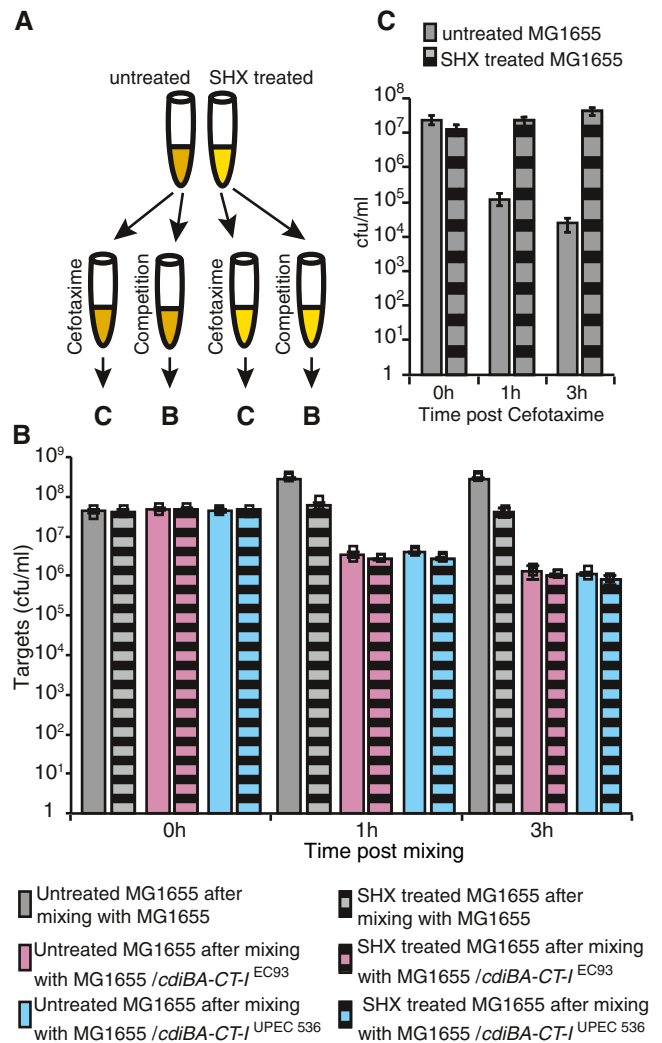

Figure 3. CdiA toxins affect antibiotic-tolerant and growing cells alike.

MG1655 cells treated with serine hydroxamate (SHX) were used to measure antibiotic tolerance or survival in competitions.

A   Overview of the experiment. Cells grown to exponential phase are split and are either untreated (solid bars) or SHX-treated (striped bars) for 15 min. After treatment, cells are split again and tested in competitions (B) or for antibiotic tolerance (C).

B   Average survival of untreated (solid bars) or SHX-treated (striped bars) MG1655 target cells after co-culturing with empty vector (grey bars), plasmid-encoded *cdiBA-CT-I*[EC93] (pink bars)- or *cdiBA-CT-I*[UPEC536] (blue bars)-positive inhibitor cells. Bars display surviving cfu/ml (n = 3).

C   Average survival of untreated (grey bars) or SHX-treated (striped bars) MG1655 cells after 0, 1 and 3 h of CEF treatment (n = 9 and 5 respectively).

Data information: Error bars represent s.e.m. and *n*-values indicate biological replicates. Scales are logarithmic (B, C).
Source data are available online for this figure.

growing cells. Lon protease was activated by SHX treatment for 1 h, to trigger the stringent response. The starvation protocol resulted in degradation of the CdiI immunity proteins in the wild type, but not in the protease-deficient strain (Fig 4D), thus suggesting that Lon can degrade CdiI upon induction of the stringent response (Appendix Fig S1B).

CdiA toxins induce the stringent response

Similarly to type II TA modules, the CdiI immunity protein seems to be degraded in cells with increased levels of (p)ppGpp. To investigate if CdiA toxins themselves induce the stringent response as has been observed for some type II TA toxins (Germain *et al*, 2013), the C-terminal toxin of CdiA[EC93] was cloned on plasmid and expressed from an arabinose-inducible promoter in a strain where the (p) ppGpp-regulated protein RpoS was fused to mCherry (Maisonneuve *et al*, 2013). The alarmone (p)ppGpp has been shown to promote RpoS stability by prevention of protein degradation and is also required for maintaining basal level *rpoS* expression (Hirsch & Elliott, 2002; Bougdour & Gottesman, 2007). To verify that this new construct actually provided toxicity and transient growth arrest as observed with delivered toxins above, the cells were tested for antibiotic tolerance. Exponentially growing cells with the toxin plasmid (pAra-CdiA-CT[EC93]) or empty vector were induced with arabinose for 15 min after which the inducer was removed and the cells were resuspended in fresh media supplemented with glucose to repress further expression of the toxin. Viability was monitored in the presence or absence of CIP through plating and colony counting (Fig 5A). Intracellular over-expression of the CdiA-CT[EC93] resulted in ~10% survival after antibiotic exposure (Figs 5A and 7C).

However, a large fraction (90%) of cells overexpressing CdiA-CT[EC93] did not resume growth after toxin induction was terminated (Fig 5A), suggesting irreversible damage to the cells. A large fraction of *cdiI*-negative cells targeted by CdiA toxins also never resume growth (drop in cfu/ml at mixing in Figs 1B and EV3A). In both of these set-ups, the cells experiencing the toxic effect of CdiA lack the *cdiI* gene and are therefore unable to relieve the toxicity by producing more CdiI. Thus, to resume growth these cells must degrade the CdiA toxins produced/delivered and it is possible that the cells unable to resume growth were not able to degrade all CdiA toxins.

To facilitate screening of many individual cells (100 cells/ sample), mCherry fluorescence was visualized in individual cells using a microfluidics device (representative image in Fig 5B). Quantification of the fluorescent signal showed that cells with empty vector (wild type or Δ*relA*Δ*spoT*) had a background fluorescence of about 1,500 units mCherry fluorescence already at the beginning of the experiment (Appendix Table S1). Cells expressing CdiA-CT[EC93] showed a 3,500-unit increase in mCherry fluorescence 1.5 h after arabinose addition, whereas the empty vector control remained at 1,500 units mCherry fluorescence (Fig 5C). To verify that the observed increase in RpoS levels was dependent on activation of the stringent response, the experiment was repeated in a Δ*relA*, Δ*spoT* strain, that is, lacking both (p)ppGpp synthases. In cells unable to
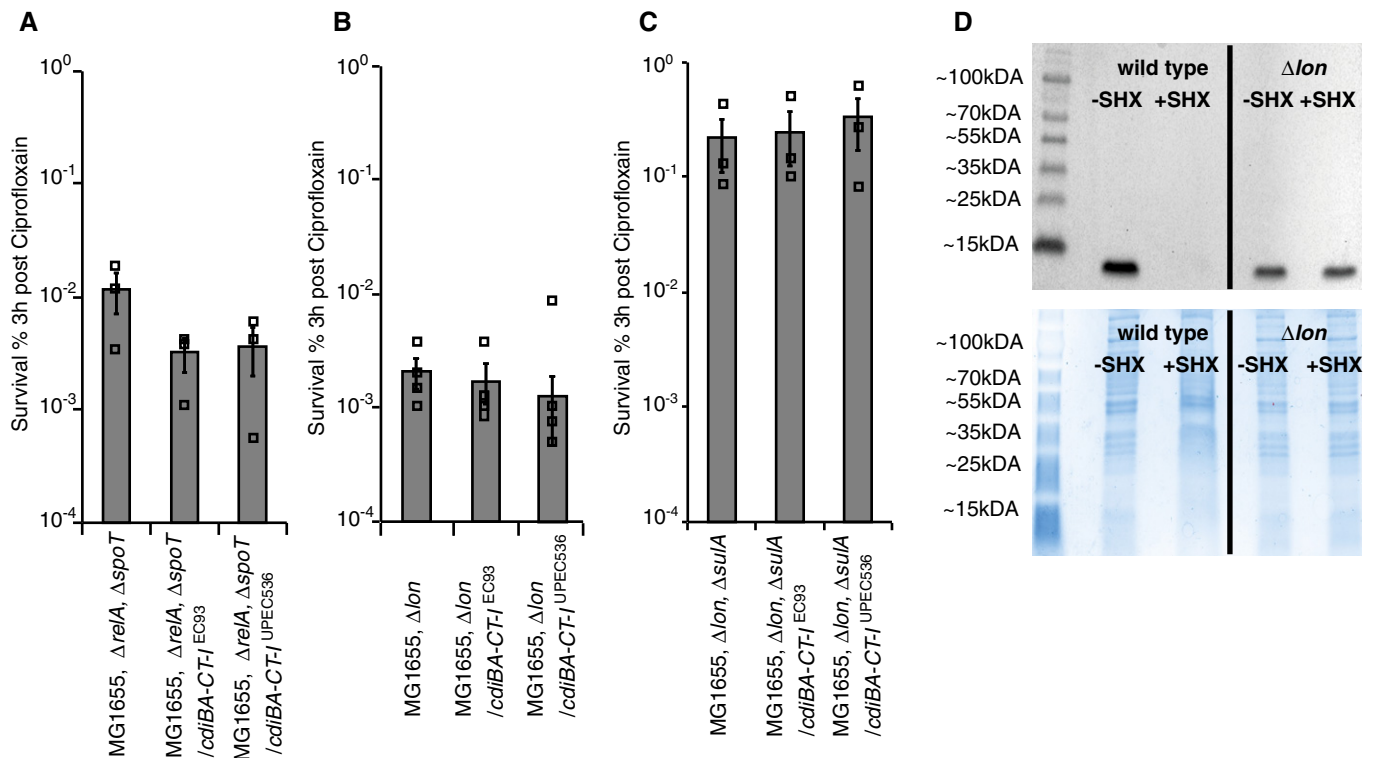

Figure 4. CdiI immunity is degraded by the Lon protease.

Average survival of exponentially growing *Escherichia coli* cells after 3 h of CIP treatment.

A–C (A) Δ*relA*, Δ*spoT*, (B) Δ*lon*, (C) Δ*lon*, Δ*sulA* cells after 3 h of CIP treatment (*n* = 3 for Δ*relA*, Δ*spoT*, 4 for Δ*lon* and 3 for Δ*lon*, Δ*sulA*). Scales are logarithmic.

D Immunoblot analysis of UPEC 536 CdiI-HA protein (14.8 kDa) stability in the presence and absence of Lon protease before and after SHX treatment for 1 h. The lower panel shows the corresponding Coomassie-stained SDS–PAGE gel as a volume loading control.

Data information: Error bars represent s.e.m. and *n*-values indicate biological replicates.
Source data are available online for this figure.

produce (p)ppGpp, only a small increase of 1,000 units mCherry fluorescence could be observed 1.5 h after arabinose induction in the toxin-expressing strain, suggesting that most of the increase observed in wild-type cells was through (p)ppGpp. In line with this, cells expressing the CdiA^{EC93} toxin from an arabinose-inducible promoter showed a 3.5-fold increase in ppGpp levels as compared to cells with an empty vector (done by thin-layer chromatography; Fig 5D and Appendix Fig S9).

Even though our persister experiment suggested that over-expression of the C-terminal toxin inside of cells could have similar outcome as toxin delivery, the large number of toxins produced could have additional effect on the cell. To test if also delivered toxins induce the stringent response in targeted cells, we used flow cytometry. To be able to separate targeted cells (lacking CdiI) from delivering cells (with the plasmid-encoded *cdiBA-CT-I*^{EC93}), we constructed reporter strain with either native BamA or BamA^{Sty} that constitutively expresses RFP from the chromosome (*galK*::RFP-*cat*). These strains were transformed with a reporter plasmid where the P*osmY* RpoS-regulated promoter (Yim *et al*, 1994) was fused to BFP (Appendix Fig S10). These target reporter cells were mixed with delivering cells expressing *cdiBA-CT-I*^{EC93}, and BFP fluorescence was observed in the RFP$^+$ population after 1 h (Fig 6A). Interestingly, ~3% of the reporter cells with cognate *E. coli* BamA showed BFP fluorescence after 1 h of co-incubation with CDI$^-$ positive cells. In contrast, < 0.1% of the reporter cells with non-cognate *Salmonella* BamA (BamA^{Sty}) were BFP$^+$ (Fig 6B). In addition, also reporter cells with BamA from either species mixed with CDI-negative cells also showed <0.1% BFP$^+$ events (Fig 6A and B). To compare the number of RpoS-activated cells with survival to antibiotics, we treated the cells as described above and added CIP to the mix. A similar sized fraction, ~3%, of the reporter cells expressing cognate BamA^{Eco} survived 1 h of CIP treatment, whereas only 0.01% survival was observed in the non-cognate BamA^{Sty} reporter and control strains (Fig 6C). Taken together, our results show that CdiA-CT^{EC93} increases (p)ppGpp levels in cells experiencing toxicity, suggesting that cell-to-cell variations in (p)ppGpp levels could also be due to contact-dependent toxins and not only due to intrinsic stochastic events as suggested previously (Maisonneuve *et al*, 2013). Thus, delivery of CDI toxins can contribute to the induction of the stringent response, which in turn entails degradation of CdiI immunity protein. These data suggest a feedforward cycle where amplification of a signal can result in growth arrest in an all-or-none manner.

CdiA toxins induce growth arrest by two distinct pathways

Induction of the stringent response results in decelerated growth of the affected cell. If the toxic activity of CdiA increases cellular (p)ppGpp levels, it is possible that the observed growth arrest is mediated by the stringent response. However, the toxic effects of the CdiA toxins alone, dissipating the proton motive force (CdiA^{EC93}; Aoki *et al*, 2009), and degrading tRNAs (CdiA^{UPEC536}) (Aoki *et al*, 2010; Diner *et al*, 2012), should be able to arrest growth by depleting ATP levels and arresting translation, respectively. To investigate if cells unable to induce stringent response responded similar to the CdiA toxins, we used the above-described construct for over-expression of CdiA-CT^{EC93} and a previously described construct for over-expression of CdiA-CT^{UPEC536} (pCH450::*cdiA-CT-I*^{UPEC536}-DAS; Diner

et al, 2012) from arabinose-inducible promoters. Cloning of the C-terminal toxin from UPEC 536 (and many other CdiA-CTs) alone results in immediate toxicity and growth arrest of the expressing cell and is therefore not possible. Instead, a degradation tag is attached
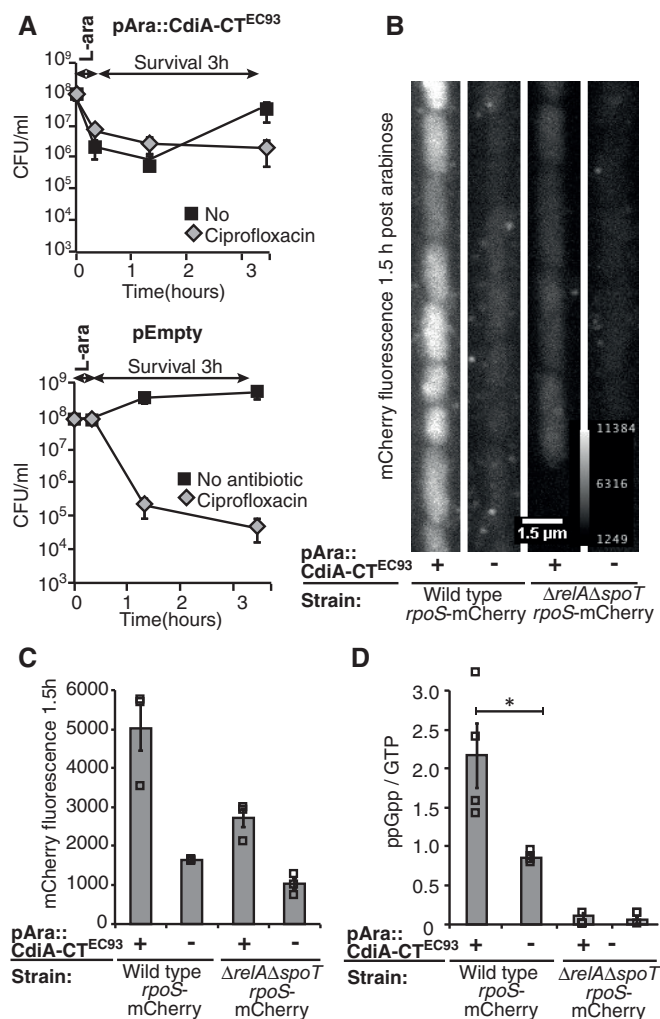

Figure 5. CdiA toxins induce the stringent response.

A   Average cfu/ml of MG1655 cells with a chromosomal RpoS-mCherry fusion and with pAra::CdiA-CT^{EC93} (upper graph) or empty vector (lower graph) after 15 min of ʟ-arabinose induction followed by washing and either no (black squares) or CIP (grey diamonds) treatment (*n* = 3 and 5 for CIP and no antibiotic series, respectively).

B, C   Cells from A were loaded in a microfluidics device after the 15-min ʟ-ara induction and mCherry fluorescence was measured using fluorescent microscopy after 1.5 h. (B) A representative image of the wild-type or *ΔrelAΔspoT* cells with a chromosomal RpoS-mCherry fusion grown with empty or CdiA-CT^{EC93} vector. Scale bar is 1.5 μm. (C) Average mCherry fluorescence of the wild-type or *ΔrelAΔspoT* cells with a chromosomal RpoS-mCherry fusion grown with empty or CdiA-CT^{EC93} vector (*n* = 3).

D   Average ratio of ppGpp/GTP in wild-type or *ΔrelAΔspoT* cells with empty or CdiA-CT^{EC93} plasmid after ʟ-arabinose induction (*n* = 4 and 3 for WT and *ΔrelAΔspoT* strains, respectively).

Data information: Error bars represent s.e.m. and *n*-values indicate biological replicates. Statistical significance was determined using Mann–Whitney *U*-test. Scales are logarithmic in (A) and linear in (C, D). *$P < 0.05$.
Source data are available online for this figure.

to the CdiI immunity protein, resulting in fast degradation of CdiI upon induction of expression, entailing growth arrest. Cells with CdiA-CT^{EC93} or CdiA-CT^{UPEC536} plasmids were induced with arabinose for 15 min in cells able (wild type) or unable ($\Delta relA$, $\Delta spoT$) to induce stringent response. The growth of cells lacking *relA* and *spoT* was not arrested as rapidly as in wild-type cells upon expression of CdiA toxins (Fig 7A and B). As a consequence, these cells did not survive antibiotic treatment to the same extent as wild-type cells with toxin (Fig 7C). To control that $\Delta relA$, $\Delta spoT$ cells express similar amount of protein upon arabinose induction as wild-type cells, a plasmid carrying the dsRed protein under an arabinose-inducible promoter (Helaine *et al*, 2010) was used. $\Delta relA$, $\Delta spoT$ and wild-type cells produced dsRed fluorescent protein similarly upon arabinose induction (Fig 7D). Thus, it is likely that CdiA toxins stop the growth of targeted cells through inducing stringent response in addition to their toxic activity. Taken together, CdiA toxins can mediate growth arrest even in cells unable to induce the stringent response

when expressed at very high levels. However, in populations of cells with CDI loci, where the toxin molecules have to outnumber the CdiI immunity molecules, the ability to induce stringent response is absolutely essential for increasing the non-growing fraction of cells through a Lon-mediated feedforward mechanism of growth arrest (Fig 4A).

Discussion

In this paper, we show that CDI can contribute to the generation of persisters in bacterial populations. Since its discovery, CDI has been considered an advanced competition machinery used in antagonistic bacterial interactions. However, there are two features of CDI that are puzzling: (i) why is delivery of toxin limited to cells of the same species, when the ability to inhibit the growth of others would provide an even greater advantage, and (ii) what is the purpose of
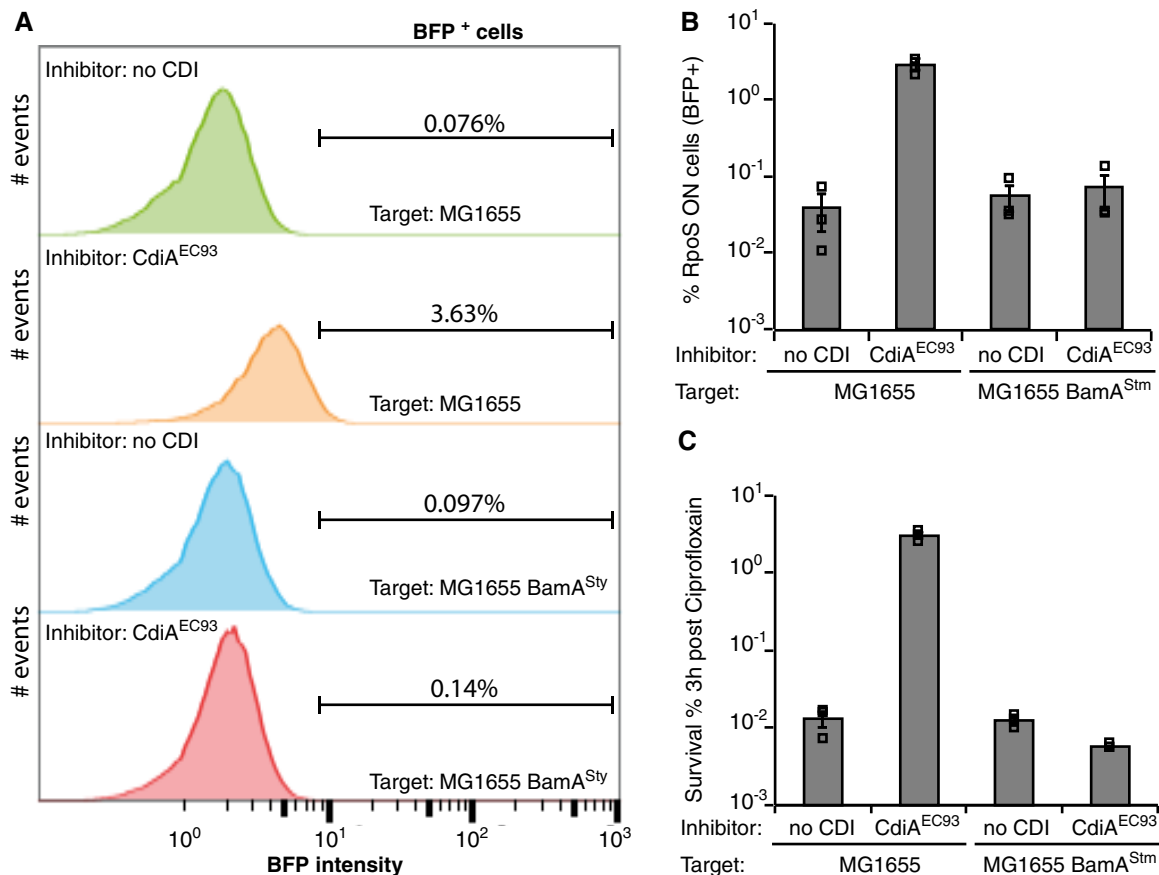

Figure 6. Delivery of CdiA-CT^{EC93} induces stringent response in receiving cells.

MG1655 cells with *cdiBA-CT-I*^{EC93} on a plasmid were co-cultured with RFP$^+$ MG1655 cells with a plasmid where the RpoS-regulated P*osmY* promoter was cloned upstream of BFP. The number of BFP$^+$ cells in the RFP$^+$ population was investigated using flow cytometry.

A   A representative image of flow cytometry data from the experiment analysed in FlowJo. Inhibitors in each experiment are indicated in the top left corner and targets in the right bottom corner. Gating for BFP is indicated with a line, and the % of BFP$^+$ events are shown above the line.

B   Average BFP$^+$ cells in the RFP$^+$ population (*n* = 3).

C   Average survival of the RFP$^+$ target population (CAM^R) after 3 h of CIP treatment (*n* = 3).

Data information: Error bars represent s.e.m. and *n*-values indicate biological replicates. Scales are logarithmic (B, C).
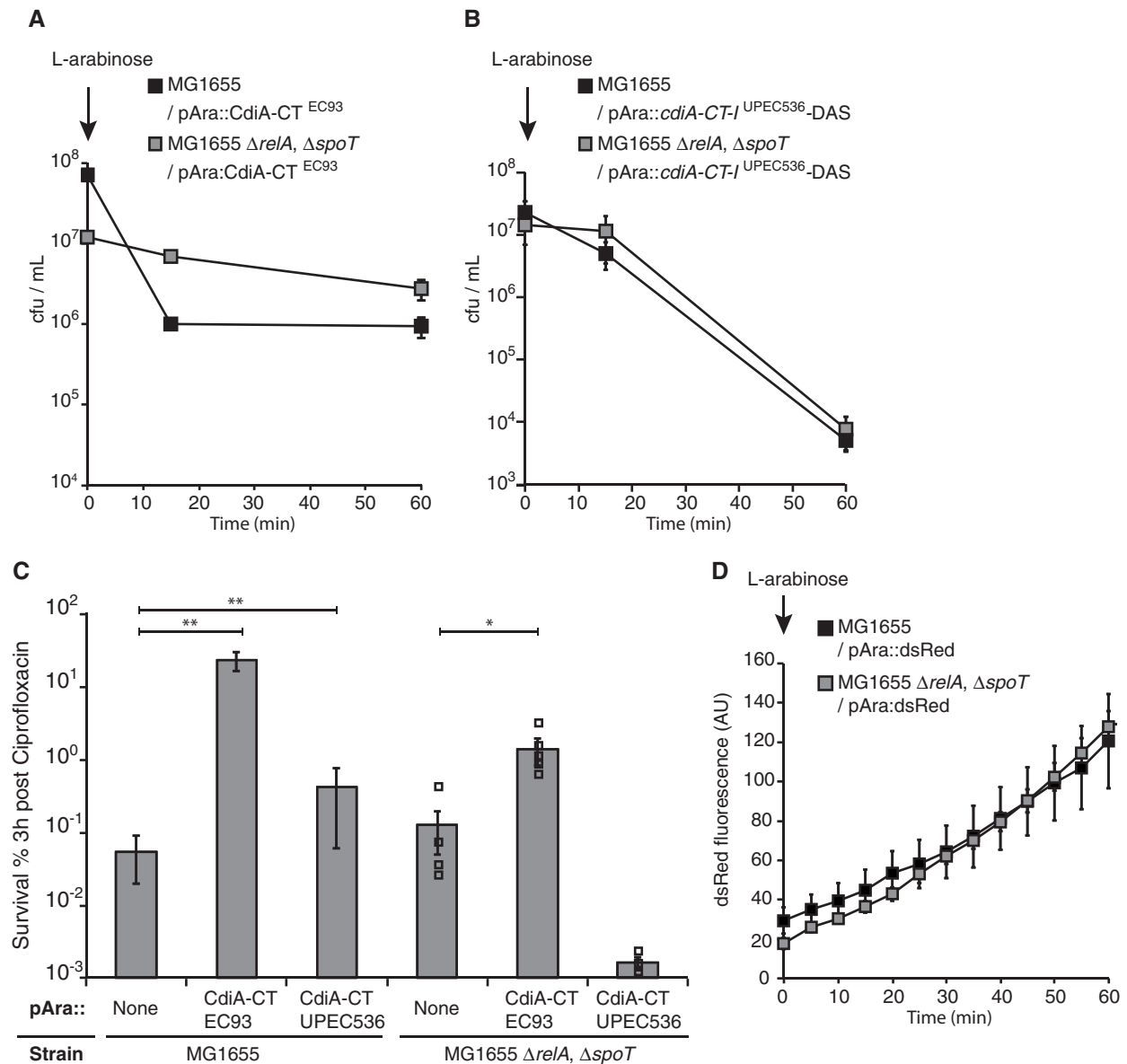Source data are available online for this figure.

Figure 7. CdiA toxins require stringent response to mediate growth arrest and antibiotic tolerance.

A, B Average cfu/ml of MG1655 wild-type or Δ*relA*Δ*spoT* cells with (A) pAra::CdiA-CT^{EC93} (*n* = 3 and 5 for WT and Δ*relA*Δ*spoT*, respectively) or (B) pAra::CdiA-CT-I^{UPEC536}-DAS plasmid after 15 min of ʟ-arabinose treatment followed by washing and resuspension in LB (*n* = 3).

C Average survival of the MG1655 wild type or Δ*relA*Δ*spoT* with empty, pAra::CdiA-CT^{EC93} or pAra::CdiA-CT-I^{UPEC536}-DAS plasmid after 3 h of CIP treatment. (*n* = 9, 6, 5, 4, 5 and 3).

D Average dsRed fluorescence in MG1655 wild-type (black squares) or Δ*relA*Δ*spoT* (grey squares) cells with pAra::mCherry plasmid after 15 min of ʟ-arabinose treatment followed by washing and resuspension in LB (*n* = 4).

Data information: Error bars represent s.e.m. and *n*-values indicate biological replicates. Statistical significance was determined using Mann-Whitney *U*-test. Scales are logarithmic for (A–C) and linear for (D).
Source data are available online for this figure.

delivering CDI toxins between immune cells? The evolutionary benefit of creating phenotypic diversity in a clonal bacterial population could be one of the explanations to why a system that specifically intoxicates cells of the same genotype would evolve.

A remaining question concerns why such a mechanism should be contact-dependent and require external delivery, that is why is it not sufficient that the toxin is produced from inside the cell as

with conventional TA systems? A possible explanation is that, as a bet-hedging strategy, it would be wasteful to create many persisters when the population density is low, since sacrificing the growth of many cells delays the expansion of the population. On the other hand, it is likely beneficial to form a higher fraction of persisters in dense populations where there are many cell-to-cell contacts, since there are sufficiently many cells that can carry

population expansion forward even with a significant non-growing fraction. In support of this hypothesis, CDI-expressing cells do not exhibit increased persister frequencies at low cell densities (10^7 cfu/ml; Fig 8A and B). Furthermore, bacteria in dense populations such as biofilms or in stationary phase display increased tolerance to antibiotics compared to exponentially growing planktonic cells (Spoering & Lewis, 2001; Keren et al, 2004a; Maisonneuve et al, 2013; Gutierrez et al, 2017). In addition, repeated exposure to antibiotics rapidly select for mutations that increase the fraction of persisters in stationary phase cultures (Van den Bergh et al, 2016), suggesting that increasing the fraction of non-growing cells at high cell densities is a good strategy for survival. However, in biofilms and in stationary phase, nutrient access is limited, making it difficult to distinguish whether it is population density per se or nutrient availability that affects persister frequency under these conditions. In our experiments, both high- and low-density cells are in exponential phase and treated otherwise identically, allowing us to show that population density per se affects CDI-mediated persister formation.

Bacteria could also regulate growth in response to increasing population density through other social interactions, for example, quorum sensing. Indeed, Pseudomonas aeruginosa, Streptococcus mutans and E. coli form increased frequencies of persisters in response to quorum sensing signals (acyl-homoserine-lactone (AHL), stress-inducible pheromone peptide (CSP) and indole, respectively) (Moker et al, 2010; Leung & Levesque, 2012; Vega et al, 2012). Somewhat surprising, one of these molecules, indole, also promotes persister formation in S. typhimurium, a bacterium that does not produce indole itself, suggesting that density-dependent persister formation through indole allows determination of cell density per se rather than functioning as a bet-hedging strategy.

Clearly, several mechanisms are in place to increase the fraction of persisters in the population as a response to increasing population densities, supporting the notion that it is more beneficial to create non-growing cells when there are many cells of the same genotype.

Persisters form also in unstressed exponentially growing populations, although at lower frequencies than at high cell density or during stress. Two different models suggest that stochastic variation in the levels of ATP or (p)ppGpp in individual cells results in a subpopulation of cells that reaches ATP or (p)ppGpp concentrations that promote growth arrest (Maisonneuve et al, 2013; Shan et al, 2017). However, the mechanism causing variation in ATP or (p)ppGpp levels in individual cells is unknown. Our results demonstrate that CDI toxins can cause variations in (p)ppGpp levels between individual cells through cell-to-cell contacts. In addition, the CdiA-CT^{EC93} is an ionophore toxin, which creates pores in the inner membrane of Gram-negative bacteria, dissipating the proton motive force and thus depleting ATP levels in the targeted cells (Aoki et al, 2009). Thus, at least one of the CdiA toxins should change ATP levels in the cells that sense the toxic effect, suggesting that CDI can cause variation in ATP levels between individual cells. In conclusion, our results suggest that when an exponentially growing population of isogenic cells with CDI systems reaches high cell density, random cell-to-cell interactions create subpopulations of cells in which the toxin molecules outnumber the immunity molecules. In these cells, the toxic effect of the CdiA toxin is sensed, resulting in initiation of the stringent response and a feedforward cycle where Lon degrades the remaining CdiI protein, eventually promoting growth arrest.

In addition to antagonistic interactions, CDI was recently suggested to promote biofilm formation and other community-associated behaviours in Burkholderia thailandensis through contact-dependent signalling (Garcia et al, 2016). Moreover, P. aeruginosa cells lacking CDI systems show differential gene expression (swarming and cyanide production) and altered virulence when compared to CDI-positive cells (Melvin et al, 2017). In these studies, the delivery of a CdiA toxin between CDI immune cells was associated with altered gene expression, but how this would mechanistically be achieved remains to be answered. Based on our findings, it is likely that CdiA toxin delivery to a subpopulation of cells where the CDI immunity protein is degraded would alter gene expression in the affected cell, creating population heterogeneity in terms of gene expression, rather than a homogenous change in all cells. If so, the changes in gene expression observed in these studies (Garcia et al, 2016; Melvin et al, 2017) would be an average of the population and greatly underestimate the changes in gene expression in individual cells. Though the CdiA toxin-immunity pair in B. thailandensis and P. aeruginosa may regulate gene expression through a different mechanism, the notion that CDI could cause heterogeneity by changing gene expression in bacterial populations is intriguing and should be investigated further.

Though first discovered in E. coli, CDI systems have been found in most bacteria (Aoki et al, 2010; Poole et al, 2011; Koskiniemi et al, 2013, 2014, 2015; Beck et al, 2014; Mercy et al, 2016). Even so, new classes of CDI toxins like those encoded by the maf-genes in Neisseria gonorrhea (Jamet et al, 2015) are still being discovered, suggesting CDI systems to be even more widespread than we know. Finally, other classes of bacteriostatic toxins, like some colicins (Sakai et al, 2015) and Type VI secretion effectors (Whitney et al,
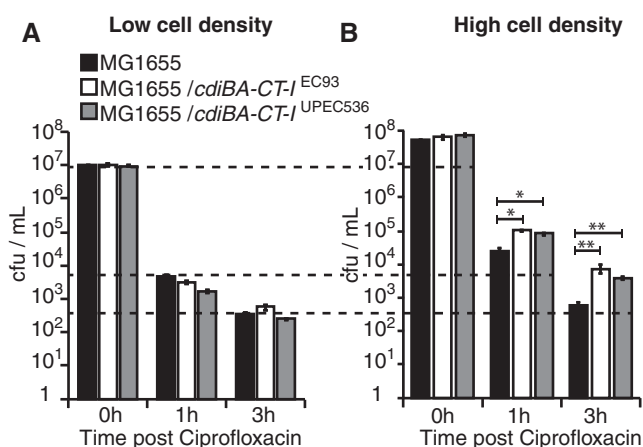

Figure 8. Population density-dependent persister formation.

A, B Average cfu/ml of exponentially growing MG1655 cells with empty (black bars), cdiBA-CT-I^{EC93} (white bars) and cdiBA-CT-I^{UPEC536} (grey bars) plasmids after treatment with CIP for 3 h. Cells at (A) low (~10^7) or (B) high (~10^8) confluence were taken from the same exponentially growing culture, centrifuged and resuspended in PBS with CIP ($n = 5$). Viable cfu/ml at 0, 1 and 3 h after centrifugation are shown. Error bars represent s.e.m. and n-values indicate biological replicates. Statistical significance was determined using Mann-Whitney U-test. Scales are logarithmic. *$P < 0.05$, **$P < 0.01$.

Source data are available online for this figure.

2015), could also in principle contribute to inter-bacterial induction of persister formation at high cell densities. Thus, cell-to-cell contact-mediated delivery of bacterial toxins could be a common bet-hedging mechanism used for creating population density-dependent heterogeneity.

Materials and Methods

All experiments were performed semi-blinded, using a number instead of the genotype as indicator of the strains included in each experiment. For all main experiments, at least three biological replicates were used to ensure reproducibility. No samples were excluded from the analysis.

Strains and growth conditions

The bacterial strains used in this study were derived from *E. coli* MG1655 (Appendix Table S2). Cells were grown in Luria-Bertani broth (LB) and incubated at 37°C/200 rpm shaking unless stated otherwise. When applicable, antibiotics were added to the growth media as follows: ampicillin (AMP) 100 mg/l, chloramphenicol (CAM) 12.5 mg/l and kanamycin (KAN) 50 mg/l, ciprofloxacin (CIP) 0.1 mg/l (10× MIC) and cefotaxime (CEF) 10 mg/l (MG1655 and UPEC 536 strains) or 40 mg/l (EC93 strain) (10× MIC for respective strains).

Construction of plasmids and chromosomal constructs

Gene deletions and chromosomal constructs were made by Lambda red recombination as described previously (Datsenko & Wanner, 2000) or retrieved from the Keio collection (Baba *et al*, 2006). Plasmids were constructed with conventional restriction digest, overlapping extension PCR or through Gibson assembly (New England Biolabs, USA). All mutations were moved to clean background after construction. Markers were moved between strains using P1 transduction, and moved constructs were verified using PCR with primers that annealed outside of the locus (Appendix Table S3). All constructs used in this study were verified by sequencing. Please check the supplemental material for detailed description of the constructed plasmids and chromosomal constructs used in this study.

Antibiotic tolerance assays

The cells were grown overnight in LB supplemented with appropriate antibiotics. Cells were diluted 1:100 in LB and grown until $OD_{600} \sim 0.3$; 1 ml of cell culture was harvested by centrifugation ($6,000 \times g$ for 3 min) and the supernatant removed before resuspending cells in 1 ml of 1× PBS. After resuspension, the number of viable target cells was determined by plating on LB plates. CEF or CIP was added to the cells, followed by incubation at 37°C/200 rpm shaking. At 1 and 3 h, the number of viable colony-forming units was determined by plating. Bacterial survival in the population was calculated as the ratio of viable cells at 1 h or 3 h compared to the number of cells at 0 h. Statistical significance was determined using Mann–Whitney *U*-test, which is suitable for comparing data with small sample size of unknown distribution.

Antibiotic tolerance after co-culturing with cells expressing CdiA toxins

Cells were grown to $OD_{600} \sim 0.3$ as mentioned above. Inhibitor and target cells were mixed 10:1, and the viable target cell counts were obtained by plating on LB plates containing the appropriate antibiotics to separate target cells from inhibitors. Cells were mixed for 15 min at 37°C/200 rpm shaking, and 1 ml was then harvested by centrifugation ($3,300 \times g$ for 3 min) and subjected to the antibiotic tolerance assay as described before with the difference that viable target cell counts were obtained by plating on LB plates containing the appropriate antibiotics to separate target cells from inhibitors. Bacterial survival in these populations was calculated as the ratio of viable cells at 1 and 3 h compared to the number of cells after 15 min of co-culturing with inhibitor cells.

Antibiotic-tolerant cells in competitions with cells expressing CdiA toxins

Bacteria were grown to an $OD_{600} \sim 0.3$, and 1 ml of target cells was harvested by centrifugation ($3,300 \times g$, 3 min) in an Eppendorf tube. Cells were resuspended in 1 ml LB and were either treated or not treated with 1 g/l SHX for 15 min at 37°C/200 rpm shaking. At this point, the cultures were split and were either treated with CEF or mixed 1:10 with inhibitor cells grown to an OD_{600} of ~0.3. The number of viable colony-forming units was determined as above.

Antibiotic tolerance after expression of CdiA-CTs from plasmids

For induction of toxin from the arabinose-inducible promoter, spent LB was used as LB contains residual sugar from yeast extract, which we found represses arabinose-inducible promoters. Spent LB was obtained from *E. coli* MG1655 cells grown to $OD_{600} \sim 0.5$ in LB by centrifugation (to remove cells) and filtering through 0.2-μm filters (for sterilization). For over-expression of CdiA-CT^{UPEC536}, we used a previously published construct (Diner *et al*, 2012) in which the CdiI immunity protein was fused to a degradation tag (CdiA-CT-I^{UPEC536}-DAS). Upon arabinose induction, both CdiA-CT^{UPEC536} and CdiI^{UPEC536} are produced, but CdiI will be degraded, resulting in growth arrest.

Cells encoding toxin under an arabinose-inducible promoter were grown overnight in LB broth supplemented with 1% glucose and 100 mM KH_2PO_4/K_2HPO_4 to repress leaky expression of toxin and to maintain pH ~ 7.5, respectively. Cells were diluted 1:500 and grown to $OD_{600} \sim 0.3$ at 37°C/200 rpm shaking. For over-expression of toxin, cells were resuspended in spent LB supplemented with 0.2% L-arabinose. After 15 min at 37°C/200 rpm shaking, the cells were harvested again and resuspended in LB broth supplemented with 1% glucose and 100 mM KH_2PO_4/K_2HPO_4 (to repress further expression of toxin) before subjected to the standard antibiotic tolerance assay described above.

Measurement of *in vivo* ppGpp levels by thin-layer chromatography (TLC)

Cells were grown to $OD_{600} \sim 0.05$ as described for CdiA-CT expression from plasmid. Cells were labelled with ^{32}P (orthophosphate

($H_3{}^{32}PO_4$), NEX053H005MC, PerkinElmer) to a 100 µCi/ml final concentration. After three to four generations of growth, at OD_{600} of 0.25–0.3, cells were centrifuged and resuspended in spent LB + 0.02% L-arabinose. After 15 min, D-glucose was added to 0.1% to terminate induction, and 0.5 ml of culture was harvested. Cells were resuspended in 1 ml 0.9% NaCl and washed by centrifugation three times. Pellets were resuspended in 200 µl 0.9% NaCl, and 200 µl of 20% formic acid was added to lyse the cells. Cell lysates were kept at −20°C. Cell debris was removed by centrifugation at 10,000 *g* for 5 min, and 20 µl of supernatant was loaded onto a TLC PEI Cellulose membrane (Merck, Germany). As a size marker, 0.2 µM of non-radioactive ppGpp (TriLink Biotechnologies, San Diego, USA) was applied. Chromatography was performed in 1.5 M KH_2PO_4 (pH 3.0) (modified from Schneider *et al*, 2003). The unlabelled ppGpp marker was visualized under UV-light. The membrane was dried, and labelled nucleotides were visualized on a PhosphorImager (Molecular Dynamics), quantified with ImageQuant software, version 4.2a (Molecular Dynamics). Ratios of ppGpp/GTP were calculated to normalize ppGpp content to the number of cells as described previously (Denapoli *et al*, 2013; Benoist *et al*, 2015).

Time-lapse microscopy

To investigate induction of stringent response, cells carrying either the empty vector (pBAD33) or the CdiA-CT^{EC93} under an arabinose-inducible promoter (pSK008) were transferred into wild-type MG1655 cells carrying *rpoS* fused to mCherry (Maisonneuve *et al*, 2013). Cells were grown to $OD_{600} \sim 0.3$ as described for CdiA-CT^{EC93} expression from plasmid. At this point, cells were diluted 1:500 one more time and grown to $OD_{600} \sim 0.3$ to dilute out excess RpoS-mCherry protein produced in stationary phase. To express CdiA-CT^{EC93}, the cells were resuspended in spent LB (see description above) supplemented with 0.2% L-arabinose to induce expression from the arabinose-inducible promoter for 15 min at 37°C/200 rpm shaking. Cells were diluted 1:50 in induction medium and loaded onto a PDMS-glass microfluidic device constructed for live cell imaging (Baltekin *et al*, 2017). The cells were imaged in fluorescence (to detect cellular mCherry expression levels) and bright field channels (to locate the cells for data analysis) using a Nikon Ti-E microscope with a Nikon Plan Apo Lambda 100× Oil immersion objective (NA 1.45), an Andor iXon3 897 EMCCD camera, and a stage incubator set to 37°C. Fluorescent microscopy employed a 561 nm DPSS-laser (Coherent) at 445 W/cm^2 in the sample plane and an exposure time of 100 ms. The dichroic mirror was zt561rdc (Chroma), and the emission filters HQ565LP (Chroma), 561NF (Chroma), and 561 nm Razor Edge Long Pass (Semrock). More than 100 cells per strain per replicate were randomly selected in bright field. Average cell fluorescence was collected from a 49 px^2 (0.123 µm^2) square region in the middle of the selected cell. Background fluorescence was measured from the cell-free region between the cell traps. Background value times 0.7 was subtracted from the cell fluorescence value. The factor of 0.7 was used to account for the lower background fluorescence in the cell traps region compared to the region in between the traps. Data analysis is performed by custom developed algorithm in MATLAB.

Expanded View for this article is available online.

Conflict of interest

The authors declare that they have no conflict of interest.

References

Ackermann M (2015) A functional perspective on phenotypic heterogeneity in microorganisms. *Nat Rev Microbiol* 13: 497–508

Amato SM, Orman MA, Brynildsen MP (2013) Metabolic control of persister formation in *Escherichia coli*. *Mol Cell* 50: 475–487

Amato SM, Brynildsen MP (2015) Persister heterogeneity arising from a single metabolic stress. *Curr Biol* 25: 2090–2098

Aoki SK, Pamma R, Hernday AD, Bickham JE, Braaten BA, Low DA (2005) Contact-dependent inhibition of growth in *Escherichia coli*. *Science* 309: 1245–1248

Aoki SK, Malinverni JC, Jacoby K, Thomas B, Pamma R, Trinh BN, Remers S, Webb J, Braaten BA, Silhavy TJ, Low DA (2008) Contact-dependent growth inhibition requires the essential outer membrane protein BamA (YaeT) as the receptor and the inner membrane transport protein AcrB. *Mol Microbiol* 70: 323–340

Aoki SK, Webb JS, Braaten BA, Low DA (2009) Contact-dependent growth inhibition causes reversible metabolic downregulation in *Escherichia coli*. *J Bacteriol* 191: 1777–1786

Aoki SK, Diner EJ, de Roodenbeke CT, Burgess BR, Poole SJ, Braaten BA, Jones AM, Webb JS, Hayes CS, Cotter PA, Low DA (2010) A widespread family of polymorphic contact-dependent toxin delivery systems in bacteria. *Nature* 468: 439–442

Baba T, Ara T, Hasegawa M, Takai Y, Okumura Y, Baba M, Datsenko KA, Tomita M, Wanner BL, Mori H (2006) Construction of *Escherichia coli* K-12 in-frame, single-gene knockout mutants: the Keio collection. *Mol Syst Biol* 2: 2006.0008

Balaban NQ, Merrin J, Chait R, Kowalik L, Leibler S (2004) Bacterial persistence as a phenotypic switch. *Science* 305: 1622–1625

Baltekin O, Boucharin A, Tano E, Andersson DI, Elf J (2017) Antibiotic susceptibility testing in less than 30 min using direct single-cell imaging. *Proc Natl Acad Sci USA* 114: 9170–9175

Beck CM, Morse RP, Cunningham DA, Iniguez A, Low DA, Goulding CW, Hayes CS (2014) CdiA from *Enterobacter cloacae* delivers a toxic ribosomal RNase into target bacteria. *Structure* 22: 707–718

Beck CM, Willett JL, Cunningham DA, Kim JJ, Low DA, Hayes CS (2016) CdiA effectors from uropathogenic *Escherichia coli* use heterotrimeric osmoporins as receptors to recognize target bacteria. *PLoS Pathog* 12: e1005925

Benoist C, Guerin C, Noirot P, Dervyn E (2015) Constitutive stringent response restores viability of bacillus subtilis lacking structural maintenance of chromosome protein. *PLoS One* 10: e0142308

Bigger JW (1944) Treatment of staphylococcal infections with penicillin by intermittent sterilisation. *Lancet* 244: 497–500

Bougdour A, Gottesman S (2007) ppGpp regulation of RpoS degradation via anti-adaptor protein IraP. *Proc Natl Acad Sci USA* 104: 12896–12901

Butler T (2011) Treatment of typhoid fever in the 21st century: promises and shortcomings. *Clin Microbiol Infect* 17: 959–963

Christensen SK, Pedersen K, Hansen FG, Gerdes K (2003) Toxin-antitoxin loci as stress-response-elements: ChpAK/MazF and ChpBK cleave translated RNAs and are counteracted by tmRNA. *J Mol Biol* 332: 809–819

Christensen SK, Maenhaut-Michel G, Mine N, Gottesman S, Gerdes K, Van Melderen L (2004) Overproduction of the Lon protease triggers inhibition of translation in *Escherichia coli*: involvement of the yefM-yoeB toxin-antitoxin system. *Mol Microbiol* 51: 1705–1717

Conlon BP, Rowe SE, Gandt AB, Nuxoll AS, Donegan NP, Zalis EA, Clair G, Adkins JN, Cheung AL, Lewis K (2016) Persister formation in *Staphylococcus aureus* is associated with ATP depletion. *Nat Microbiol* 1: 16051

Datsenko KA, Wanner BL (2000) One-step inactivation of chromosomal genes in *Escherichia coli* K-12 using PCR products. *Proc Natl Acad Sci USA* 97: 6640–6645

Denapoli J, Tehranchi AK, Wang JD (2013) Dose-dependent reduction of replication elongation rate by (p)ppGpp in *Escherichia coli* and *Bacillus subtilis*. *Mol Microbiol* 88: 93–104

Diner EJ, Beck CM, Webb JS, Low DA, Hayes CS (2012) Identification of a target cell permissive factor required for contact-dependent growth inhibition (CDI). *Genes Dev* 26: 515–525

Durfee T, Hansen AM, Zhi H, Blattner FR, Jin DJ (2008) Transcription profiling of the stringent response in *Escherichia coli*. *J Bacteriol* 190: 1084–1096

Elowitz MB, Levine AJ, Siggia ED, Swain PS (2002) Stochastic gene expression in a single cell. *Science* 297: 1183–1186

Garcia EC, Perault AI, Marlatt SA, Cotter PA (2016) Interbacterial signaling via Burkholderia contact-dependent growth inhibition system proteins. *Proc Natl Acad Sci USA* 113: 8296–8301

Germain E, Castro-Roa D, Zenkin N, Gerdes K (2013) Molecular mechanism of bacterial persistence by HipA. *Mol Cell* 52: 248–254

Gutierrez A, Jain S, Bhargava P, Hamblin M, Lobritz MA, Collins JJ (2017) Understanding and sensitizing density-dependent persistence to quinolone antibiotics. *Mol Cell* 68: 1147–1154.e3

Helaine S, Thompson JA, Watson KG, Liu M, Boyle C, Holden DW (2010) Dynamics of intracellular bacterial replication at the single cell level. *Proc Natl Acad Sci USA* 107: 3746–3751

Hirsch M, Elliott T (2002) Role of ppGpp in rpoS stationary-phase regulation in *Escherichia coli*. *J Bacteriol* 184: 5077–5087

Jamet A, Jousset AB, Euphrasie D, Mukorako P, Boucharlat A, Ducousso A, Charbit A, Nassif X (2015) A new family of secreted toxins in pathogenic *Neisseria* species. *PLoS Pathog* 11: e1004592

Jones AM, Garza-Sanchez F, So J, Hayes CS, Low DA (2017) Activation of contact-dependent antibacterial tRNase toxins by translation elongation factors. *Proc Natl Acad Sci USA* 114: E1951–E1957

Keren I, Kaldalu N, Spoering A, Wang Y, Lewis K (2004a) Persister cells and tolerance to antimicrobials. *FEMS Microbiol Lett* 230: 13–18

Keren I, Shah D, Spoering A, Kaldalu N, Lewis K (2004b) Specialized persister cells and the mechanism of multidrug tolerance in *Escherichia coli*. *J Bacteriol* 186: 8172–8180

Korch SB, Henderson TA, Hill TM (2003) Characterization of the hipA7 allele of *Escherichia coli* and evidence that high persistence is governed by (p)ppGpp synthesis. *Mol Microbiol* 50: 1199–1213

Koskiniemi S, Lamoureux JG, Nikolakakis KC, t'Kint de Roodenbeke C, Kaplan MD, Low DA, Hayes CS (2013) Rhs proteins from diverse

bacteria mediate intercellular competition. *Proc Natl Acad Sci USA* 110: 7032–7037

Koskiniemi S, Garza-Sanchez F, Sandegren L, Webb JS, Braaten BA, Poole SJ, Andersson DI, Hayes CS, Low DA (2014) Selection of orphan Rhs toxin expression in evolved *Salmonella enterica* serovar typhimurium. *PLoS Genet* 10: e1004255

Koskiniemi S, Garza-Sanchez F, Edman N, Chaudhuri S, Poole SJ, Manoil C, Hayes CS, Low DA (2015) Genetic analysis of the CDI pathway from *Burkholderia pseudomallei* 1026b. *PLoS One* 10: e0120265

Kuroda A, Nomura K, Ohtomo R, Kato J, Ikeda T, Takiguchi N, Ohtake H, Kornberg A (2001) Role of inorganic polyphosphate in promoting ribosomal protein degradation by the Lon protease in *E. coli*. *Science* 293: 705–708

Leung V, Levesque CM (2012) A stress-inducible quorum-sensing peptide mediates the formation of persister cells with noninherited multidrug tolerance. *J Bacteriol* 194: 2265–2274

Maisonneuve E, Shakespeare LJ, Jorgensen MG, Gerdes K (2011) Bacterial persistence by RNA endonucleases. *Proc Natl Acad Sci USA* 108: 13206–13211

Maisonneuve E, Castro-Camargo M, Gerdes K (2013) (p)ppGpp controls bacterial persistence by stochastic induction of toxin-antitoxin activity. *Cell* 154: 1140–1150

Melvin JA, Gaston JR, Phillips SN, Springer MJ, Marshall CW, Shanks RMQ, Bomberger JM (2017) *Pseudomonas aeruginosa* contact-dependent growth inhibition plays dual role in host-pathogen interactions. *mSphere* 2: e00336–17

Mercy C, Ize B, Salcedo SP, de Bentzmann S, Bigot S (2016) Functional characterization of pseudomonas contact dependent growth inhibition (CDI) systems. *PLoS One* 11: e0147435

Moker N, Dean CR, Tao J (2010) *Pseudomonas aeruginosa* increases formation of multidrug-tolerant persister cells in response to quorum-sensing signaling molecules. *J Bacteriol* 192: 1946–1955

Moyed HS, Bertrand KP (1983) hipA, a newly recognized gene of *Escherichia coli* K-12 that affects frequency of persistence after inhibition of murein synthesis. *J Bacteriol* 155: 768–775

Ozbudak EM, Thattai M, Kurtser I, Grossman AD, van Oudenaarden A (2002) Regulation of noise in the expression of a single gene. *Nat Genet* 31: 69–73

Poole SJ, Diner EJ, Aoki SK, Braaten BA, t'Kint de Roodenbeke C, Low DA, Hayes CS (2011) Identification of functional toxin/immunity genes linked to contact-dependent growth inhibition (CDI) and rearrangement hotspot (Rhs) systems. *PLoS Genet* 7: e1002217

Pu Y, Zhao Z, Li Y, Zou J, Ma Q, Zhao Y, Ke Y, Zhu Y, Chen H, Baker MA, Ge H, Sun Y, Xie XS, Bai F (2016) Enhanced efflux activity facilitates drug tolerance in dormant bacterial cells. *Mol Cell* 62: 284–294

Ruhe ZC, Low DA, Hayes CS (2013a) Bacterial contact-dependent growth inhibition. *Trends Microbiol* 21: 230–237

Ruhe ZC, Wallace AB, Low DA, Hayes CS (2013b) Receptor polymorphism restricts contact-dependent growth inhibition to members of the same species. *MBio* 4: e00480–13

Ruhe ZC, Townsley L, Wallace AB, King A, Van der Woude MW, Low DA, Yildiz FH, Hayes CS (2015) CdiA promotes receptor-independent intercellular adhesion. *Mol Microbiol* 98: 175–192

Ruhe ZC, Nguyen JY, Chen AJ, Leung NY, Hayes CS, Low DA (2016) CDI systems are stably maintained by a cell-contact mediated surveillance mechanism. *PLoS Genet* 12: e1006145

Ruhe ZC, Nguyen JY, Xiong J, Koskiniemi S, Beck CM, Perkins BR, Low DA, Hayes CS (2017) CdiA effectors use modular receptor-binding domains to recognize target bacteria. *MBio* 8: e00290–17

Sakai F, Sugita R, Chang JW, Ogawa T, Tsumadori N, Takahashi K, Hidaka M, Masaki H (2015) Transfer-messenger RNA and SmpB mediate bacteriostasis in *Escherichia coli* cells against tRNA cleavage. *Microbiology* 161: 2019–2028

Schneider DA, Murray HD, Gourse RL (2003) Measuring control of transcription initiation by changing concentrations of nucleotides and their derivatives. *Methods Enzymol* 370: 606–617

Shan Y, Brown Gandt A, Rowe SE, Deisinger JP, Conlon BP, Lewis K (2017) ATP-dependent persister formation in *Escherichia coli*. *MBio* 8: e02267–16

Smith AS, Rawlings DE (1998) Efficiency of the pTF-FC2 pas poison-antidote stability system in *Escherichia coli* is affected by the host strain, and antidote degradation requires the lon protease. *J Bacteriol* 180: 5458–5462

Spoering AL, Lewis K (2001) Biofilms and planktonic cells of *Pseudomonas aeruginosa* have similar resistance to killing by antimicrobials. *J Bacteriol* 183: 6746–6751

Tosa T, Pizer LI (1971) Effect of serine hydroxamate on the growth of *Escherichia coli*. *J Bacteriol* 106: 966–971

Traxler MF, Summers SM, Nguyen HT, Zacharia VM, Hightower GA, Smith JT, Conway T (2008) The global, ppGpp-mediated stringent response to amino acid starvation in *Escherichia coli*. *Mol Microbiol* 68: 1128–1148

Tsuchimoto S, Nishimura Y, Ohtsubo E (1992) The stable maintenance system pem of plasmid R100: degradation of PemI protein may allow PemK protein to inhibit cell growth. *J Bacteriol* 174: 4205–4211

Van den Bergh B, Michiels JE, Wenseleers T, Windels EM, Boer PV, Kestemont D, De Meester L, Verstrepen KJ, Verstraeten N, Fauvart M, Michiels J (2016) Frequency of antibiotic application drives rapid evolutionary adaptation of *Escherichia coli* persistence. *Nat Microbiol* 1: 16020

Van Melderen L, Bernard P, Couturier M (1994) Lon-dependent proteolysis of CcdA is the key control for activation of CcdB in plasmid-free segregant bacteria. *Mol Microbiol* 11: 1151–1157

Vazquez-Laslop N, Lee H, Neyfakh AA (2006) Increased persistence in *Escherichia coli* caused by controlled expression of toxins or other unrelated proteins. *J Bacteriol* 188: 3494–3497

Veening JW, Smits WK, Kuipers OP (2008) Bistability, epigenetics, and bet-hedging in bacteria. *Annu Rev Microbiol* 62: 193–210

Vega NM, Allison KR, Khalil AS, Collins JJ (2012) Signaling-mediated bacterial persister formation. *Nat Chem Biol* 8: 431–433

Verstraeten N, Knapen WJ, Kint CI, Liebens V, Van den Bergh B, Dewachter L, Michiels JE, Fu Q, David CC, Fierro AC, Marchal K, Beirlant J, Versees W, Hofkens J, Jansen M, Fauvart M, Michiels J (2015) Obg and membrane depolarization are part of a microbial bet-hedging strategy that leads to antibiotic tolerance. *Mol Cell* 59: 9–21

Webb JS, Nikolakakis KC, Willett JL, Aoki SK, Hayes CS, Low DA (2013) Delivery of CdiA nuclease toxins into target cells during contact-dependent growth inhibition. *PLoS One* 8: e57609

Whitney JC, Quentin D, Sawai S, LeRoux M, Harding BN, Ledvina HE, Tran BQ, Robinson H, Goo YA, Goodlett DR, Raunser S, Mougous JD (2015) An interbacterial NAD(P)(+) glycohydrolase toxin requires elongation factor Tu for delivery to target cells. *Cell* 163: 607–619

Yim HH, Brems RL, Villarejo M (1994) Molecular characterization of the promoter of osmY, an rpoS-dependent gene. *J Bacteriol* 176: 100–107